

Noise - How important is it in application of MEMS and MOEMS?

A. Selvarajan

Department of Electrical Communication Engineering

Indian Institute of Science, Bangalore 560012, India.

Tel: +91-080-394 2283 Fax: +91-080-360 0563

Email: rajan@ece.iisc.ernet.in

ABSTRACT

There are various types of noise sources such as shot noise, thermal noise and flicker noise in electronic devices, quantum noise in photonic devices and noise due to Brownian motion in the case of MEMS which limit the performance of the systems based on these devices. In communication applications, noise causes degradation in SNR or BER leading to loss or errors in the received signal. In the case of sensor systems, noise poses a problem in terms of the minimum detectable quantity such as pressure or rotation rate or radiation field. In this paper first an overview of noise sources, noise modeling and analysis is given. Simulation results for some specific MOEM devices are presented. A comparative study of the performance of MEMS versus MOEMS for the same or similar application is also highlighted.

Keywords: Noise, analysis, simulation, MEMS, MOEMS

1. INTRODUCTION

Noise sources and their influence on system performance is a well-researched topic and there exists rich literature on this topic. Nevertheless with the current interest in functionally integrated systems such as system-on-a-chip wherein one tries to create micro- and nano- level electronic, photonic and mechanical elements on the same chip, it becomes important to understand the combined effect of the various noise terms which originate differently in different devices. Apart from the noise sources that are intrinsic to the devices (such as shot and thermal noises) there are other noise sources, which are extrinsic (such as noise due to temperature fluctuations in the ambience, pickup from external sources, unwanted feedback, RF interference from other systems, power supply fluctuations, ground currents etc.). Even if the extrinsic noise sources are avoided by proper assembly, shielding and grounding etc., the intrinsic noise sources which are due to fundamental property of the devices can be only reduced by careful design but not eliminated totally. Noise sets a limit to the minimum detectable or resolvable quantity under measurement in the case of sensors while its presence leads to degradation in SNR or BER and causes loss or errors in the received signal in communication systems.

There have been a few studies on noise issues in MEMS. Chau and Wise¹ have carried out a detailed study of noise due to Brownian motion in diaphragm type MEM pressure sensors. They have shown that the low frequency Brownian noise is very small, two to three orders of magnitude less than the thermal noise in the piezoresistive devices and various noise sources in read out circuitry. Harley and Kenny² have analyzed the influence of $1/f$ noise on piezoresistive cantilever based sensors. It was shown that annealing can reduce $1/f$ noise. Vig and Kim³ on the other hand have studied the influence of noise on the performance of MEMS based resonators. An advantage of MEMS technology is that a large number of resonators can be fabricated on a single wafer. Therefore they predict that by connecting N resonators in series a reduction in noise by a factor of \sqrt{N} can be achieved, if the noise is uncorrelated. Requirements to achieve low-noise acoustic and vibration sensors have been investigated by Bernstein et al⁴ and Gabrielson⁵. Although in recent times MOEMS have gained in importance, studies relating to noise analysis of MOEMS have not drawn the attention of many researchers. Tucker et al⁶ have studied the thermal noise and radiation pressure effects on micro Fabry-Perot etalons used as tunable filters and lasers. In this paper we present an analysis and simulation of noise in some MEMS and MOEMS. In particular noise analysis for two types of MOEM devices, a pressure sensor and an accelerometer are discussed in detail. A comparative study of the performance of MEM based pressure sensor versus MOEM based pressure sensor is also presented.

2. NOISE SOURCES AND MODELING OF NOISE

Noise is a randomly varying entity and so in the modeling of noise, first the autocorrelation function is modeled according to the random variations and then by taking its Fourier transform, the power spectral density is obtained. Shot noise, thermal noise, flicker noise and circuit noise are important electrical noise sources and the behavior of the same has been mathematically well-quantified⁷⁻¹⁰

Shot noise arises due to granularity of charges i.e. the charges come only in the multiples of the charge ‘e’ on an electron. This is very fundamental and shows up in circuit components in which current is carried by electrons having to cross a potential barrier such as in going through the base in a transistor. The auto correlation function for this type of noise can be represented as

$$R(\tau) = 2e\bar{I}\delta(\tau) \quad (1)$$

where, \bar{I} is the average current and τ represents the time interval between the current pulses. The power spectrum is given by

$$S(f) = 2e\bar{I} \quad (2)$$

The noise spectrum is flat for frequencies below $1/t_0$, t_0 is the transit time of the electron through the barrier i.e., $\sim 10^{10}$ Hz.

The **thermal noise**, also known as Johnson or Nyquist noise results from the thermal motion of electrons. This too is fundamental in nature, related to black body radiation that involves the fluctuations of electromagnetic field in thermal equilibrium. Johnson investigated the same experimentally and Nyquist proposed the theoretical model. The power spectrum for thermal noise is given by

$$S_v(f) = 4k_B T R \quad (3)$$

where k_B is Boltzman’s constant and T is the equilibrium temperature. No thermal fluctuations occur for $f > f_{\max} = k_B T/h$, where h is Plank’s constant. For room temperature, f_{\max} is 0.588GHz.

The **flicker noise** or $1/f$ noise¹¹ arises due to fluctuations of resistance of a circuit element. Unlike shot noise and thermal noise, it is not a white noise. The origin of it is mainly due to trapping and releasing of electrons. It is particularly important in devices, which rely on action at surfaces and interfaces such as FETs. The power spectrum of the flicker noise is given by

$$S_R(f) = \frac{A}{f^\alpha} \quad (4)$$

where, A is a parameter independent of f and current I, and α is a constant close to unity. Both A and α are system dependent. The voltage power spectrum, when current is constant is given by

$$S_V(f) = \frac{AI^2}{f^\alpha} \quad (5)$$

Photon noise¹²⁻¹³ occurs in semiconductor optical radiation detectors. This is same as shot noise in electronic devices. This also arises due to granularity of the photons that is received by the detector, which produces charge carriers. The noise spectrum associated with the detected electrical current is given by

$$S(f) = 2e\bar{I} \quad (6)$$

The average current \bar{I} is given by, for an incident optical power P_{in}

$$\bar{I} = R P_{in} \quad (7)$$

where, R is the responsivity of the detector and is given by

$$R = \frac{\eta e}{h\nu} \quad (8)$$

In the above equation, η is the quantum efficiency of the detector; h is the Plank’s constant and ν is the frequency of the light falling on the detector. In addition to the noise in detectors, noise associated with optical sources (lasers) such as Relative Intensity Noise (RIN), mode partition noise, etc. may become important in certain applications. The noise current associated with RIN is given by¹⁴

$$\overline{i_L^2} = RIN \overline{i_s^2} B \quad (9)$$

where i_s is the average photocurrent, and RIN is the laser noise normalized to unit bandwidth.

Mechanical–thermal noise is an important noise source in the case of MEMS. Micro mechanical devices consisting of small moving parts are subjected to random displacements due to the molecular agitation of the surrounding medium. This noise is also referred to as noise due to Brownian motion¹⁵. The mean square displacement of a mass-spring oscillator resulting from thermal agitation is given by

$$\frac{1}{2} k \overline{x^2} = \frac{1}{2} k_B T \quad (10)$$

where k is the spring constant and the associated spectrum of the noise force is given by (in units of N/√Hz)

$$F = \sqrt{4k_B T R} \quad (11)$$

where R is the mechanical resistance. The equivalent noise pressure is obtained as

$$p = \sqrt{4k_B T R_{aco}} \quad (12)$$

where $R_{acs} = R/S^2$, S is the surface area. The above case is appropriate at higher pressures. At low pressures, the molecular motion is neither spatially nor temporally correlated. In this case, the pressure fluctuation is modeled as a space-time white noise process. This is dealt with in section 3.1. The application of the above concepts to study the performance of specific MEMS and MOEMS is taken up in the following sections.

3 MEMS AND MOEMS BASED PRESSURE SENSORS

Most of the MEMS pressure sensors reported till now are either piezoresistive or capacitive type. Piezoresistive sensors have good linearity whereas capacitive sensors have good sensitivity. Piezoresistive sensors cannot operate at very high temperature, as the piezoresistivity is temperature dependent. Capacitive sensors can be operated at high temperatures, but have very less dynamic range. Both these show poor response in electromagnetically active environment. This is where MOEM sensor can play an important role since the interrogation is in the optical domain and so are immune to EMI. For a concise overview of micro mechanical pressure sensors the paper by Eaton and Smith¹⁶ may be referred.

A number of groups have also developed MOEM based pressure sensors. In the earliest reported work by Ohkawa et. al¹⁷, a novel integrated optic pressure sensor was constructed with the Mach-Zehnder structure of glass waveguides on a silicon substrate. Detecting the deformation of the thin diaphragm through MZI senses pressure. The experimentally measured half-wave pressure was 0.8×10^5 Pa. Wagner et.al¹⁸ have developed a similar MOEM sensor along with a pin detector in the same chip. They used Silicon Oxynitride waveguides in the MZI form and used He-Ne laser for interrogation. From the data presented it seems to show a half-wave pressure of 7.5 kPa. Halg¹⁹ has proposed another type of pressure sensor, where the Fabry-Perot interferometer was formed in a glass layer with a spacer on top of a micromachined silicon diaphragm. Brabender et.al²⁰ have proposed yet another type of pressure sensor which uses an integrated optical ring resonator to measure the strain induced in the micromechanical diaphragm due to applied pressure. The reported half-wave sensitivity was about 1.1×10^5 Pa. Howard et.al²¹ have developed an interferometric pressure transducer using a single fringe etalon detection scheme as intensity mode signal for a deformable silicon diaphragm. Benaissa and Nathan²² have reported design, fabrication of silicon integrated optical pressure sensor based on a micromechanical MZI. This work utilizes an anti resonant reflecting optical waveguide (ARROW), which show low loss (1dB/cm), for the IO MZI. Sensitivity of 180 μradians/Pa has been obtained with the push pull configuration. Kim, and Neikirk²³ have explored the use of a FP cavity for sensing pressure along with a SM fiber to illuminate the cavity and also collect the return light. Porte et.al²⁴ have demonstrated a pressure sensor using an imbalanced MZI over a silicon micromachined diaphragm. This sensor works in a coherence scheme, allowing linear phase readout of the signal. The wavelength shift of the transmitted spectrum of imbalanced MZI due to applied pressure, gives the sensor signal. Pressures upto 15 bar has been measured using this sensor with accuracy of 1.4%.

3.1 Noise analysis for Pressure Sensors

We now analyze the noise characteristics of some typical pressure sensors

3.2 Capacitive pressure sensor

As mentioned earlier in the case of MEMS based ultra sensitive pressure sensor the limiting performance is due to Brownian motion. A diaphragm pressure sensor is described by a displacement function with the applied pressure in terms of fourth order partial differential equation (Chau and Wise¹). This is then solved using a normal mode expansion. Apart from the usual thermal and shot noise terms in the case of MEMS it is the noise due to Brownian motion that will set the fundamental limit for ultra sensitive pressure sensors. To obtain quantitative results about the fluctuating noise pressure, the Brownian motion is treated as an ergodic random process and the mean square deflection is obtained through a Fourier transform of the autocorrelation function^{1,25}.

The mean square variation of change in capacitance is obtained as

$$\overline{(\Delta C / C_0)^2} = 0.010 \frac{1-\nu^2}{E} \frac{K}{\mu} \frac{a^2}{h^3 d^2} \quad (13)$$

From the definition of capacitive pressure sensitivity the equivalent Brownian noise pressure per unit bandwidth is obtained as

$$\overline{p_n^2} = 1.15 \frac{K}{a^2} \quad (14)$$

where $K = \sqrt{\frac{32k_B T}{\pi}} (\sqrt{m_1} P_1 + \sqrt{m_2} P_2)$, P_1 and P_2 are pressure on either side of the diaphragm and m_1, m_2 are mass of the gas on either side of the diaphragm, a is the radius, h is thickness of the diaphragm and d is the separation between the electrode forming the diaphragm and the ground with no applied pressure. This is valid at low pressures and for frequencies much below the diaphragm fundamental resonance frequency. Fig.1 shows the rms Brownian noise pressure due to surrounding air at 300⁰ K per unit bandwidth for a 7 micron thick circular diaphragm of varying radius for a capacitive pressure sensor. It is seen that the noise decreases inversely as the square of the radius of the diaphragm.

3.3 Piezoresistive pressure sensor

In some cases it is possible to obtain the fluctuating Brownian noise in a simpler way as follows. Any mechanical system in thermal equilibrium can be analyzed for mechanical-thermal noise by adding a force generator alongside each damper. From this model one can then obtain the fluctuation pressure related through an acoustic resistance⁵. The pressure fluctuation can be obtained by calculating the density of thermal-acoustic vibration modes in it as

$$S_p(f) = \frac{2\pi k T \rho f^2}{v} \quad (15)$$

where v and f are velocity and frequency of sound in the medium and ρ is the density. We apply this concept to a piezo resistive pressure sensor as follows. The sensitivity of piezoresistive pressure sensor is given by¹

$$\frac{\Delta R}{R P} = K_{piezo} \left(\frac{a}{h}\right)^2 \quad (16)$$

where K_{piezo} is a constant relating to piezoresistive coefficients. By substituting the noise pressure from (15) for at room temperatures into (16), we get the variation of $\Delta R/R$ as shown in Fig. 2 for various diaphragm radius over a 20kHz spectrum. In this example the orientation of the piezoresistor is in <110> on <100> silicon.

3.4 Opto-Mechanical Pressure Sensor

Fabry-Perot interferometric detection method has been extensively used in many fiber optic sensing systems. There are two ways of using the Fabry-Perot – intensity variation as a result of perturbation or frequency/wavelength shift due to perturbation. The intensity change in the relatively high pressure region can be measured in terms of number of fringes that shift under the influence of applied pressure. The detection can thus be simpler. On the other hand, wavelength shift can offer fine resolution. However the required spectrum analyzer is more complex and expensive. We consider here the case of wavelength shift as an example as outlined in⁶

$$\Delta\lambda = \frac{x(P)\lambda}{d} \quad (17)$$

where x is the deflection due to the applied pressure, d is the cavity length and λ is the wavelength of light. The wavelength shift due to noise pressure at room temperature for different radius of the diaphragm is shown in Fig 3.

4. NOISE IN MICROMACHINED ACCELEROMETERS

As outlined in section 2 the mechanical-thermal noise is given in terms of a force relating to R_{acs} where R_{acs} is a mechanical damping per unit area. From this we can then obtain the mechanical thermal noise induced acceleration⁵

$$a = \frac{\sqrt{4KTR_{acs}}}{Mg} \quad g / \sqrt{Hz} \quad (18)$$

where M is the proof mass, $g=9.8 \text{ m/sec}^2$, R_{acs} is the thermo acoustic resistance which is calculated using¹ as

$$R_{acs} = \frac{A^2 \rho f^2}{V} \quad N.s/m \quad (19)$$

Where A is the surface area of the proof mass, ρ is the density of the surrounding medium, V is the velocity and f is the frequency of sound in the gas medium. (18) can also be expressed in terms of Q as

$$a = \frac{1}{g} \sqrt{\frac{4KT \omega_0}{MQ}} \quad g / \sqrt{Hz} \quad (20)$$

It can be seen that, to achieve low noise we need high Q and a large mass that is limited by the dimension of the microstructure. The noise equivalent acceleration as a function of temperature and Q are shown in Fig 4.

4.1 Opto-Mechanical Accelerometer

Combination of Integrated Optics with MEMS to realize micro machined devices for sensing, signal processing and communication applications offers flexibility and versatility as also novel architectures. Broadly there are two types of MOEMS: Free-Space and Guided wave devices depending on whether light propagates through air or through a wave guiding structure such as glass fiber or planar and channel integrated optics waveguides. Applications of Free-Space devices include Communication, Signal Processing, Projection Display, Scanning System, Optical Disk Pickup and Adaptive Optic Systems, while applications involving waveguide elements are various types of Sensors and Optical Interconnects.

Examples of Guided wave MOEMS include various types of interferometers such as Mach-Zehnder or Fabry-Perot, Directional Coupler, Bragg Grating and other well known optical guided wave devices. The light propagating through waveguide based elements as above is modified by a movable mechanical element such as cantilever or diaphragm, under the influence of an external perturbation such as force, vibration etc. Unlike free space devices where only the direction of propagation of light changes, in guided wave devices the optical radiation may under go a change in amplitude, phase or polarization. This makes it more versatile and highly sensitive compared to electrical capacitance or resistance measurement systems. Some published work relating to micro-machined optically addressed accelerometers can be seen in²⁶⁻³⁰.

We now consider a Micro-Opto-Electro-Mechanical (MOEM) accelerometer consisting of an integrated optic Mach-Zehnder interferometer one arm (the sensing arm) of which is placed on to a micro machined diaphragm or a bridge and the other arm serves as a reference. In this case the analysis consists of determining changes in phase shift due to acceleration-induced refractive index change as also optical path length variation in the Mach-Zehnder interferometric sensor. A noise analysis is carried out to study the fundamental performance limit due to noise for different sensor configurations³⁰.

In the case of a MZI used as an optical detection device the output intensity is given by

$$I = \frac{I_0}{2} (1 + \cos \Delta\phi) \quad (21)$$

where I_0 is the intensity of light from the laser diode and $\Delta\phi$ is acceleration induced phase shift given by

$$\Delta\phi = \beta\Delta L + \int_L \delta\beta dL \quad (22)$$

where L is the active length of the sensor arm and β is the propagation constant of the guided mode. Here, $\beta = n_{\text{eff}} k_0$, $k_0 = 2\pi/\lambda$, λ is the wavelength of light. The first and second terms in (22) represent the phase shift arising from the acceleration induced path elongation and the photo-elastic effect, respectively. These can be easily evaluated from well known considerations and we obtain the total phase shift as³⁰

$$\Delta\phi = \frac{2\pi}{\lambda} \frac{n}{n_{\text{eff}}} \int \Delta n_{TE}(y, z) dz + \frac{2\pi}{\lambda} n_{\text{eff}} \Delta L \quad (23)$$

$\Delta\phi$ is simulated for three different proof-mass structures with variation of aspect ratio, thickness of substrate and acceleration. When the photon noise is the limiting noise the minimum detectable phase change is given by

$$\Delta\phi_{\text{min}} = \sin^{-1} \left(\sqrt{\frac{2qB}{I_0}} \right) \quad (24)$$

Thus the minimum detectable phase change depends on the output optical power falling on the detector as shown in Fig.5. For an incident optical power of 1 μW the minimum detectable phase change is found to be about 5.6 μradian .

The induced phase change due to refractive index variation and MZI path length variation is simulated for cantilever and bridge type configurations and the results are shown in Fig. 6a and 6b. It is observed that the minimum detectable acceleration for cantilever type and bridge type configurations is better than 10 μg . The sensitivity of bridge type proof mass with higher b/a values is better than the cantilever type proof mass, where b is the length and a is the width of the proof mass.

5. CONCLUSION

In this paper a noise analysis and simulation results for different types of pressure and acceleration sensors are presented. Typical noise pressure (due to Brownian motion) in the case of capacitive pressure sensor is seen to be $10^{-7} \mu\text{m Hg}/\sqrt{\text{Hz}}$ for a diaphragm pressure sensor of radius 800 μm . In the case of MEMS accelerometers it is found that to achieve low noise it is necessary to have high Q and a large proof mass. The acceleration measurement using MOEM device consisting of Mach-Zehnder interferometric integrated optic structure on two types of silicon proof masses (cantilever and diaphragm) are analyzed. Simulation results show that it is possible to detect a minimum acceleration of about 10 μg as per the present simulation. In this study primarily Brownian motion noise and photon noise were considered. Further investigation taking into account other types of noise sources as well is necessary to arrive at definite conclusion regarding the relative importance of different types of noise sources.

ACKNOWLEDGEMENT

The author wishes to thank AICTE for providing the Emeritus Fellowship. He also wishes to thank Dr. T. Srinivas, Mr P. K. Pattnaik, Mr. T. Madan and Mr. V. Naveen for assistance in the preparation of the manuscript. The author wishes to thank NPSM/B-SMART for providing financial support for travel to present the paper at SPIE's Smart Structures and Materials Conference, 2 - 6 March 2003, San Diego, California, USA.

REFERENCES

1. Hin-Leung Chau and K.D.Wise, "Scaling limits in batch fabricated in silicon pressure sensors", IEEE ED **34**(4), pp.850-858, 1987. Also, Hin-Leung Chau and K.D.Wise, "Noise due to Brownian motion in ultrasensitive solid-state pressure sensors", IEEE ED **34**(4), pp. 859-865, 1987.
2. J.A.Harley and T.W Kemmy, "1/f noise considerations for the design and process optimisation of piezoresistive cantilevers", IEEE/ASME JI of MEMS, Vol.9, No.2, pp. 226-235, 2001.

3. J.R.Vig and Y.Kim, "Noise in microelectromechanical system resonators", IEEE Trans. On Ultrasonics, Ferroelectrics and frequency control, Vol.46, No.6, pp.1558-1565, 1999.
4. J. Bernstein, R. Miller, W. Kelley, P. Ward. "Low-noise MEMS vibration sensor for geophysical applications", Technical Digest, Solid-State Sensor and Actuator Workshop, Hilton Head Island, SC, June 8-11, pp. 55-58, 1998.
5. T.B. Gabrielson, "Mechanical-thermal noise in micromachined acoustic and vibration sensors", IEEE Trans. Electron Devices ED **40**, 903-909, 1999.
6. R. S. Tucker, D. M. Baney and C. A. Flory, "Thermal Noise and Radiation Pressure in MEMS", IEEE JI. on Selected Topics in Quantum Electronics, **8**(2), pp.88-97, 2002.
7. J.B.Johnson, "Thermal agitation of electricity in conductors", Phys. Rev. **32**, pp. 97-109, 1928.
8. H.Nyquist, "Thermal agitation of electric charge in conductors", Phys. Rev. **32**, pp.110-113, 1928.
9. H.B. Callen and T.A. Welton, "Irreversibility and generalised noise", Phys. Rev. **83**, No.1, pp. 34-40, 1951.
10. M. Gupta, "Electrical Noise: Fundamentals and Source", IEEE Press. 1977.
11. F.N. Hooge, " 1/f Noise is no surface effect", Phys Lett. A Vol.29, pp.139-140, 1969.
12. J. Muller, "Photodiodes for optical communications", Advances in Electronics and Electron Physics, **55**, 189-308, 1981.
13. P.W. Kruse, "A comparison of the limits to the performance of thermal and photon detection imaging arrays", Infrared phys. Technol., Vol **36**, pp 869-882, 1995.
14. G. P. Agrawal, "Fiber Optic Communications systems", J. Wiley, New York, 1992.
15. G.E. Uhlenbeck and L.S.Ornstein, "On the theory of the Brownian motion", Phys. Rev. Vol.36, pp.823-841, 1930.
16. W P Eaton and J H Smith, "Micromachined pressure sensors: review and recent developments", J. Smart Materials and Structures, **6**, 530-539, 1997.
17. M. Ohkawa, M. Izutsu and T. Sueta, " Integrated Optic pressure sensor on silicon substrate", Appl. Opt., Vol. **28**, No.23, pp.5153-5157, 1989.
18. C. Wagner, J. Frankenberger and P.Deimel, "Optical Pressure sensor based on a Mach-Zehnder Interferometer integrated with a lateral a-Si:H p-i-n Photodiode", IEEE PTL, Vol.5, No.10, pp.1257-1259, 1993.
19. B. Halg, "A Silicon pressure sensor with a low-cost contact less interferometric optical readout", Sensors and Actuators, Vol.30, pp.225-230, 1992.
20. G.N.De Brabander, J.T.Boyd and G. Beheim, "Integrated Optical Ring resonator with micromechanical diaphragm for pressure sensing", IEEE Photonic Technology Letters, Vol.6, No.5, pp. 671-673, 1994.
21. D.L.Howard, S.D.Collins and R.L.Smith, "A Single fringe etalon silicon pressure transducer", Sensors and Actuators, Vol.86, pp.21-25, 2000.
22. K.Benaissa and A.Nathan, "IC compatible opto-mechanical pressure sensor using Mach- Zehnder interferometry", IEEE ED, Vol. **43**, No.9, pp.1571-1581, 1996.
23. Y. Kim, and D.P.Neikirk, "Micromachined Fabry-Perot cavity pressure transducer", IEEE Photonic Technology Letters, Vol., No.12, pp.1471-1473, 1995.
24. H.Porte, V.Gorel, S.Kiryenko, J.P. Goedgebuer, W.Daniau and P.Blind, "Imbalanced Mach-Zehnder Interferometer integrated in a micro-machined silicon substrate for pressure sensor", IEEE JLT, Vol. **17**, No.2, pp.229-233, 1999.
25. A.Selvarajan and S. Anand, "Noise Analysis and a comparative study of noise in MEMS and MOEMS", Proc. of SPIE **3673**, pp.113-121, 1999.
26. A. Malki, P.Lecoy J. Marty C. Renouf and P.Ferdinant, "Optical fiber accelerometer based on a silicon micromachined cantilever", Appl. Opt., **34**(34), pp. 8014-8018, 1995.
27. Zhixiong Xiao , Min Chen, Guoying Wu, Chang Zhao, Dacheng Zhang, Yilong Hao, Guobing Zhang, and Zhihong Li "Silicon micro-accelerometer with mg resolution, high linearity and large frequency bandwidth fabricated with two mask bulk process", Sensors and Actuators **77**, 113-119, 1999.
28. K. E. Burchcham, G. N. De Brabander and J.T. Boyed, "Micromachined silicon cantilever beam accelerometer incorporating an integrated optical waveguide", in Integrated Optics and Microstructures Proc. SPIE **1793**, 12-18, 1992.
29. M.Ohkawa, M.Izutsu and T.Sueta, "Integrated optic accelerometer employing a cantilever on silicon substrate", Japanese JI. of App. Phys **28**(2), pp.287-288, 1989.
30. A. Selvarajan, J. Nayak, S. Anand and T. Srinivas, "Noise and sensitivity analysis of some MEMS and MOEMS", Indo-Japanese workshop on Microsystem Technology, Delhi, 23-25, Nov 2001.

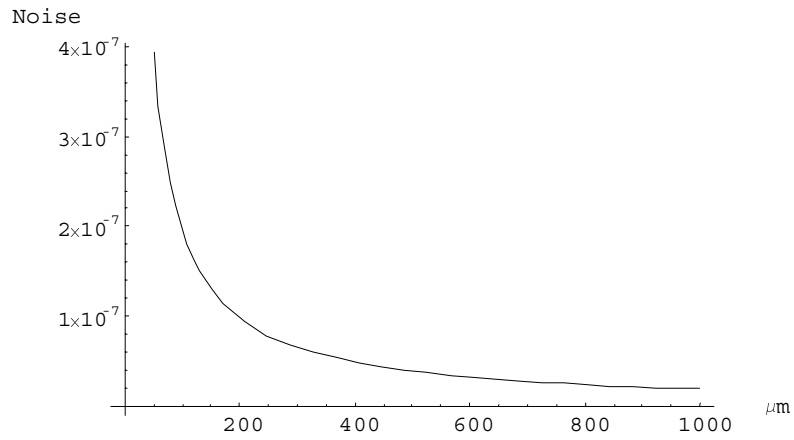


Fig.1 Noise ($\mu\text{m Hg}/\sqrt{\text{Hz}}$) due to Brownian motion vs. diaphragm radius in the case of a capacitive pressure sensor.

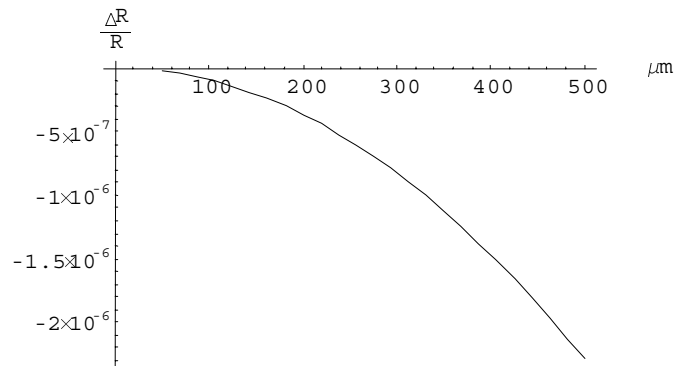


Fig.2 Resistance change due to Brownian noise pressure at room temperature vs diaphragm radius.

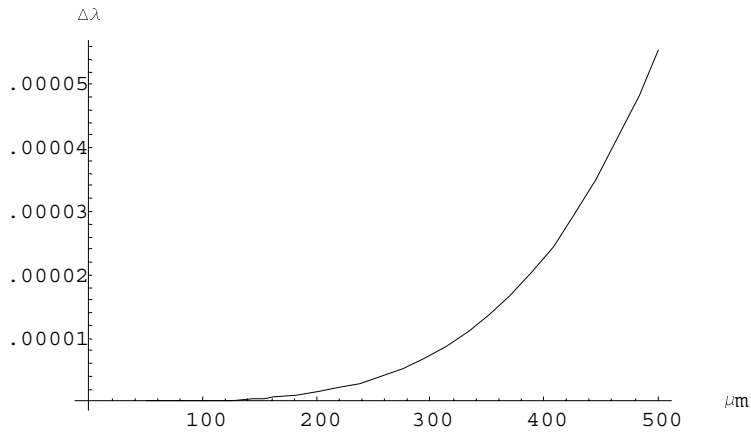


Fig. 3 Wavelength shift as a function of diaphragm radius at room temperature.

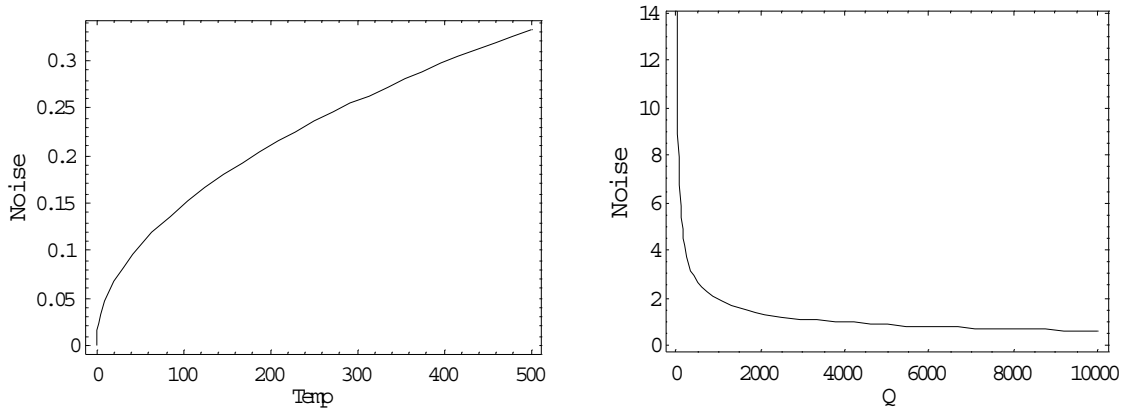


Fig 4: Acceleration Noise in $\mu\text{g}/\sqrt{\text{Hz}}$ as a function of temperature and quality factor.

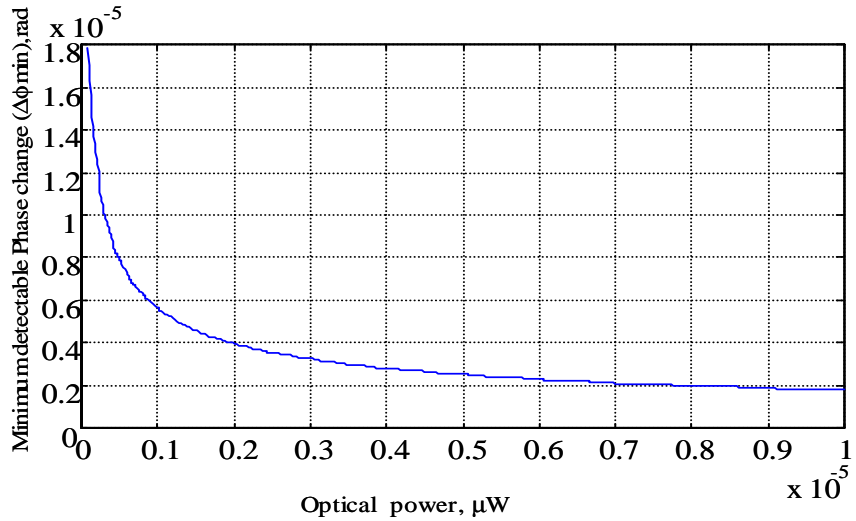


Fig.5: Minimum detectable phase change Vs optical power falling on the detector.

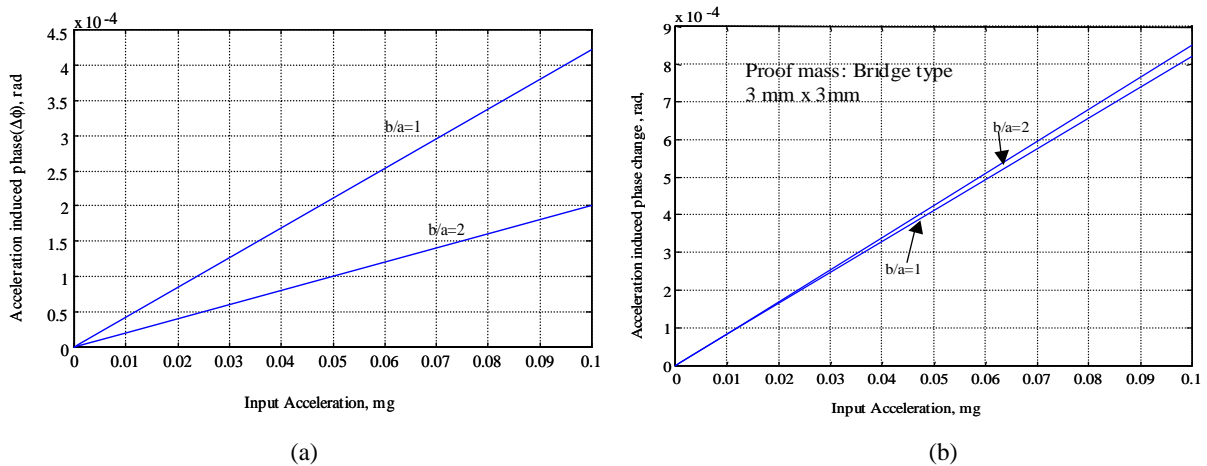


Fig.6: Induced phase change vs input acceleration: (a) Cantilever, (b) Bridge type with two fixed ends.